RSC Advances

ROYAL SOCIETY OF CHEMISTRY

www.rsc.org/advances

Graphical Abstract

Taoran Zhang,[a] Cheng Jin,[a] Lingyu Wang[a] and Qinjian Yin[a*]

[a]*Key Laboratory of Green Chemistry and Technology and College of Chemistry, Sichuan University, Chengdu, 610064, China*

We introduce a facile and novel way that describes the random amphiphilic azo copolymer to construct hollow nanospheres via hydrogen bond formation.

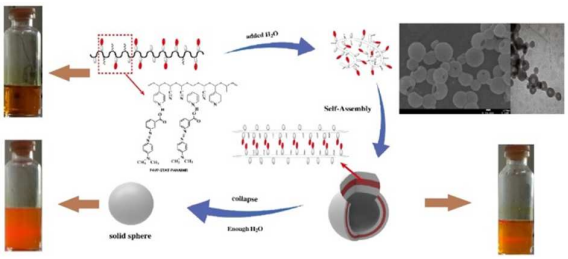

* Corresponding author: Tel.: +86 28 85418112; fax: +86 28 85412907. E-mail address: E-mail: changer@scu.edu.cn

Journal Name

RSCPublishing

ARTICLE

One-Step Synthesis of Hollow Polymeric Nanospheres: Self-Assembly of Amphiphilic Azo Polymers Via Hydrogen Bond Formation

Cite this: DOI: 10.1039/x0xx00000x

Received 00th January 2012,
Accepted 00th January 2012

DOI: 10.1039/x0xx00000x

www.rsc.org/

Taoran Zhang,[a] Cheng Jin,[a] Lingyu Wang[a] and Qinjian Yin*[a]

This article reports a facile and novel way of fabricating polymeric hollow nanospheres with azo functional groups. M-Methyl red (MMR) with a carboxyl group at the apex site could attach to random copolymer poly (acrylonitrile-*stat*-4-vinylpyridine) (denoted PAN-*stat*-P4VP), forming hydrogen-bonded brush-like polymers (HBBP) in their common solvent, tetrahydrofuran(THF). The HBBP shows unique self-assembly behavior, forming hollow nanospheres in the common solvent with the increase of water content under whisk. The size and morphology of hollow nanospheres are homogeneous and can be conveniently controlled by varying molar ratios of the copolymers to MMR and the composition of the copolymers. DLS, TEM, SEM, FTIR and UV-Vis studies demonstrated the construction and formation mechanism of the hollow nanospheres (HNSs). Compared to the conventional route to shell-cross-linked micelles and hollow spheres from the micelles made of block copolymers, the current approach has the significant advantages of avoiding chemical degradation of the core components and synthesis of block copolymers. Thus, the results clearly prove that the hollow nanospheres constructed from the random copolymers and azobenzene micromolecules are a new and promising platform for the study of hollow nanospheres in solution.

Introduction

Azobenzene-containing polymers are a fascinating class of photochromic materials because of the multitude of photoinduced effects brought by the photoisomerization of the azobenzenes.[1-5] In the preceding decades, azobenzene-containing polymers have attracted considerable attention for their unique properties, such as phase transition,[6] chromophore orientation,[7] surface-relief-grating (SRG) formation,[8] optical nonlinearity,[9] and photoinduced deformation,[10]which are caused by the trans-cis photoisomerization of azobenzenes. Azo polymers with different molecular architectures have been synthesized for various applications, that contain side-chain or main-chain azo groups and can be classified as branched, crosslinked, dendritic polymers linear, or star-like, depending on their topological structure.[11-13] The design of azo polymers with different structures has become an attractive research project.

Self-assembly of amphiphilic polymers have developed to be an efficient method to construct various matters, which have been extensively explored to obtain a variety of well-defined order structures, such as spherical micelles,[14] rod-like micelles,[15] vesicles[16] and hollow nanotubes.[17] Among them, the structures with hollow cavities have attracted much attention resulting from their unique architecture and broad applications, such as drug-delivery, catalysis and inks among others.[18-20] Nowadays, amphiphilic block copolymers, as the most well-known examples, can form a variety of hollow cavities.[21] Recently, it has been reported that hollow nanospheres (HNSs) can be determined by the relative sizes of the hydrophilic and preferential swelling of the components.[22] In contrast, the random copolymers are quite less studied due to their ill-defined properties in terms of structure control. To a large extent, whether amphiphilic random copolymers can form various hollow structures with controllable organizations is still an open question.

For this paper, we study the assembly behavior of hydrogen-bonded brush-like polymers (HBBP) consisting of a random copolymer main chain with a small molecule of azobenzene attached through hydrogen bonds.[23] Amphiphilic azo polymers can combine the photoresponsive properties of azo polymers with the self-assembling characteristics of amphiphilic polymers.[24] The general idea underlying this study stems from our long-term investigation of the "dibolck-copolymer-free strategy" in macromolecular assembly.[25] Compared with block polymers, random polymers are easy to be synthesized and their self-assemblies are also expected if appropriate design of the polymers were considered.[26] Previously, our group reported a facile method to fabricate polymeric HNSs via Ionic Self-Assembly.[27] The HNSs were formed through gradual hydrophobic aggregation of the polymeric chains in mixed aqueous-organic solvents, induced by a continuous increase of the water content. We have recently investigated that conventional copolymers are generally not homogeneous in composition at the molecular level. In RAFT polymerization processes, all chains have similar composition and are called gradient or tapered copolymers. [28] The RAFT polymerization will afford each copolymer chain with homogeneous chemical compositions. Hence, the RAFT copolymers are suitable for synthesizing in a facile and economical approach for large-scale production.[29] To our knowledge, observation and study of HNSs via self-assembly of random copolymers by the hydrogen bond formation have not been reported in the literature yet. Therefore, it is important to see if the simply designed random

HBBP could facilitate the formation of the HNSs.

Herein we document the hydrogen-bonding-assisted self-assembly of m-Methyl red (MMR), a H-donor azobenzene micromolecule, and H acceptor polymers containing pyridine repeating units: poly (acrylonitrile-*stat*-4-vinylpyridine) (PAN-*stat*-P4VP). We synthesized copolymer poly (acrylonitrile)-*stat*-poly (4-vinylpyridine) (PAN-*stat*-P4VP) in DMF via radical copolymerization according to Figure 1. Upon mixing the MMR and PAN-*stat*-P4VP in their common solvent THF, after that H_2O was added, then the blend solution turned turbid until the appearance of the faint opalescence, which indicated the formation of aggregates in the solution. It is comparable to that reported for the micelles of graft copolymer PAA-g-PS and NCCM.[30-31] DLS studies showed the aggregates to have a diameter around 500nm with a narrow distribution, as indicated by the low polydispersity index (PDI). On the other hand, we turned to track the formation mechanism of the HNSs by DLS and track the construction of hollow nanpspheres by UV-VIS .Meanwhile, the size of the aggregates increases as the molar ratio PVP/MMR decreases and a low PVP/MMR ratio corresponds to a larger aggregate. This dependence provides a simple way to adjust the dimensions of the aggregates by changing the weight ratio of the component polymers. Finally, effects of azocomplexes composition on the morphology of HNSs were discussed, and the formation mechanism of polymeric HNSs was proposed.

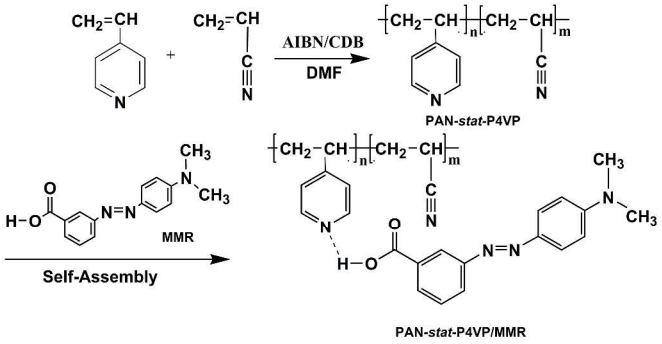

Figure 1. Reaction scheme for synthesis of statistical copolymer PAN-*stat*-P4VP, PAN and azocomplex PAN-*stat*-P4VP /MMR.

Experimental Section

Materials

4-Vinylpyridine (4VP; 95%Acros) and acrylonitrile (AN; >99%, Chengdu Kelong Chemical Reagent Co.) were dried over calcium hydride (CaH2) and then distilled under reduced pressure prior to use. Azobisisobutyronitrile (AIBN) (C.P., Chengdu Kelong Chemical Reagent Co.) was recrystallized twice using ethanol. Deionized water (resistivity > 18M_) was obtained from a millipore water purification system and was used for the following experiments. m-Methyl red (MMR) was obtained from Aladdin. All the other chemical reagents were purchased from Chengdu Kelong Chemical Reagent Co. and used as received.

Synthesis of cumyl dithiobenzoate (CDB)[32]

CDB was synthesized in yield of 30.2% according to the method described in ref. 25. According to the ^{1}H NMR spectrum of CDB, the characterization peaks are assigned as the following: d (ppm): 2.02 (6H, s, CH_3), 7.20-7.60 (8H, m, meta, *ortho*-ArH) and 7.86 (2H, m, *para*-ArH). According to the ^{13}C NMR spectrum of CDB, The characterization peaks are assigned as the following δ (ppm): 28.3, 56.5, 126.6, 128.2, 131.8, 144.2, and 146.3. The C=S signal (δ>220.0 ppm) was beyond the frequency range of the NMR spectrum. By FI-IR spectrum characterization, the characterization peaks of C=S appear at 1042 cm^{-1} and 1221 cm^{-1}.

RAFT copolymerization of 4-Vinylpyridine and acrylonitrile

RAFT copolymerization of 4-Vinylpyridine (4VP) and Acrylonitrile (AN) was performed and 2, 2'-azobisisobutyronitrile (AIBN) as initiator. 4-Vinylpyridine (10.0 mL, 93.2 mmol), acrylonitrile (6.1 mL, 93.1 mmol), CDB (0.428 g, 1.573 mmol) and AIBN (0.086 g, 0.524 mmol) were mixed together. A threeneck flask charged with 50.0 mL of dimethylformamide (DMF) was heated to reflux. Then the mixture of monomer and initiator was added dropwise over 30 min. The reaction was heated for 6 h. After that, the polymer was precipitated by pouring the whole reaction mixture into large amount of cold deionized water. A pale yellow precipitate was obtained and purified by three DMF/H_2O cycles in diethyl ether at room temperature and dried in a vacuum oven at 55 °C for 5 days.

Synthesis of PAN-*stat*- P4VP /MMR azocomplexes

Copolymer PAN-*stat*-P4VP and MMR were added to DMF solution, which monomer molar ratio (4-VP: MMR) was 1:0.4 and 1:0.9 respectively. A THF solution of 1.0g/L copolymer was prepared. Then the mixture of deionized water was added dropwise until the aqueous solution muddied.

Table.1 Molecular characterization of azocomplexes with different VP: MMR ratios.

PAN_m-*stat*-$P4VP_n$/MMR_x	4VP:AN/ ^{1}H NMR	4VP:MMR	Concentration (mg·mL^{-1})
PAN_{52}-*stat*-$P4VP_{101}$/MMR_{41}	79:150	1:0.4	1
PAN_{52}-*stat*-$P4VP_{101}$/MMR_{91}	79:150	1:0.9	1
PAN_{52}-*stat*-$P4VP_{101}$/MMR_{41}α	79:150	1:0.4	0.5
PAN_{52}-*stat*-$P4VP_{101}$/MMR_{41}β	79:150	1:0.4	1.5
PAN_{52}-*stat*-$P4VP_{101}$/MMR_{41}γ	79:150	1:0.4	2

Characterization

^{1}H NMR spectra and ^{13}C NMR were recorded by a Bruker AV II-400 NMR spectrometer at room temperature. Transmission electron micrographs (TEM) were obtained on a JEM-100CX (working voltage of 200 kV) instrument. A drop of the solution was placed onto a carbon-supported copper grid in -40 ºC vacuum by the freeze dryer for 1 h. Infrared spectra were recorded on Bruker Tensor 27 infrared spectrophotometer. Fourier transform infrared (FTIR) absorption spectra were obtained with a Bruker Tensor 27. UV-Vis spectra were recorded by Unico UV-2800A spectrophotometer from 300 nm to 600 nm at 25 ºC. To determine the size and distribution of polymeric HNSs, the system was analyzed by the dynamic light scattering instrument (DLS, Malvern Nano-ZS, and wavelength of 632.8 nm) at 25 ºC. The molecular weight and molecular weight distribution were determined on a Waters 150C gel permeation chromatography (GPC) equipped with three Ultrastyragel columns (500, 103, 104 Å) in series and RI 2414 detector at 30 ºC, and DMF was used as eluent at a flow rate of 1.0 mL min^{-1}. Scanning electron microscope (SEM) images of samples were investigated using JSM-5900LV scanning electrons microscope.

Results and Discussion

Azobenzene-containing polymers were obtained following the convergent synthetic approach depicted in Figure 1. In the first step, we synthesized copolymers, poly(acrylonitrile-*stat*-poly(4-vinylpyridine)) (denoted PAN-*stat*-P4VP) via RAFT copolymerization in DMF using CDB as a macro- RAFT agent and 2, 2-azobisisobutyronitrile (AIBN) as an initiator. PAN-*stat*-P4VP is an amphiphilic copolymer composed of hydrophilic 4-vinylpyridine units and hydrophobic acrylonitrile units. Because of the synthetic method, the hydrophobic units are randomly distributed along the polymeric chain and the polymer possesses polydispersity in both the molecular weight and the loading density of the hydrophobic units. The overall monomer molar ratio (4-VP: AN=150:79) was determined by ^{1}H NMR spectroscopy in DMSO-D6 (Figure 2). The blunt peak between 1.0 and 2.3 ppm related to the main chain (-CH_2-CH_2-) protons of PAN-*stat*-P4VP, and the 4-vinylpyridine protons of copolymer appear 6.8 and 8.3 ppm. It means that PANm-*stat*-P4VPn polymers were synthesized, where <m> and <n> represent the average number of monomer in a polymer chain, respectively. The degree of functionalization (DF) is defined as the percentage amount of 4-vinylpyridine (4-VP) units among total units. The PAN_{52}-*stat*-$P4VP_{101}$ sample used in this study has the DF of 65.79%.The weight-average molecular weight (Mw) and number-average molecular weight (Mn) are 16803 and 13421 respectively.

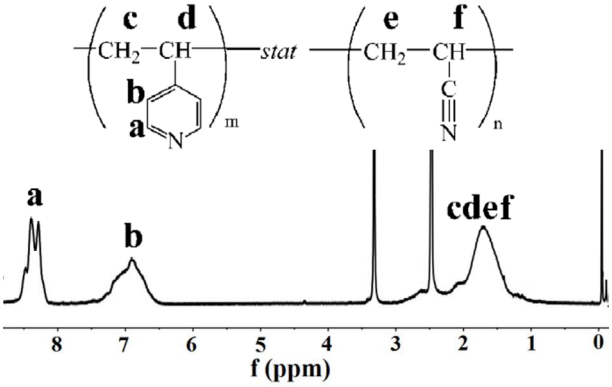

Figure 2. ^{1}H NMR spectrum of statistical copolymer PAN-*stat*-P4VP in DMSO-d6

Self-assembly of HBBP

For the hydrogen-bonded brush polymers preparation, the polymer (PAN_{52}-*stat*-$P4VP_{101}$) and MMR (molar ratio 1:0.4) were first dissolved in THF to form a homogeneous solution of azocomplexes. The initial concentration of PAN_{52}-*stat*-$P4VP_{101}$/MMR in THF was 1 mg·mL^{-1}. Azocomplexes were expected to form through hydrogen bonds between the carboxyl group at the MMR and the pyridine group of PAN_{52}-*stat*-$P4VP_{101}$ (Figure 3). The formation of the hydrogen bonds is supported by FT-IR spectroscopy measurements. Compared to the infrared spectrum (Figure 4) of PAN_{52}-*stat*-$P4VP_{101}$/MMR, MMR shows new absorption bands at 2239.3 cm^{-1}, the nitrile group (-CN) stretching vibration absorption peak in the PAN-*stat*-P4VP, which indicates that pyridine groups and MMR have mixed. The FTIR spectra of the blend solutions also qualitatively reflect the hydrogen-bonding interaction between pyridine and carboxyl as the stretching bond of carboxyl shifts from 1685.7 to 1703.1 cm^{-1} upon mixing of the two solution.[33] In other word, PAN_{52}-stat-$P4VP_{101}$/MMRx azocomplexes were synthesized by the intermolecular interactions between PAN_{52}-*stat*-$P4VP_{101}$ and MMR, where <x> represents the number of MMR in the PAN_{52}-*stat*-$P4VP_{101}$/MMRx azocomplexes.

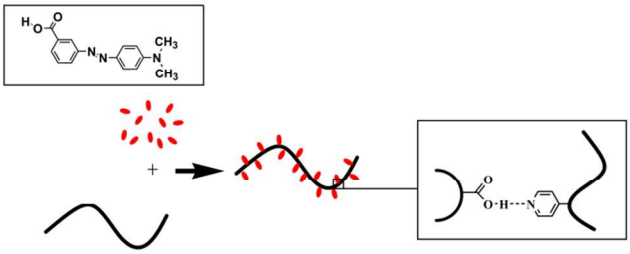

Figure 3. A schematic illustration of the formation of the H-bonded azocomplexes.

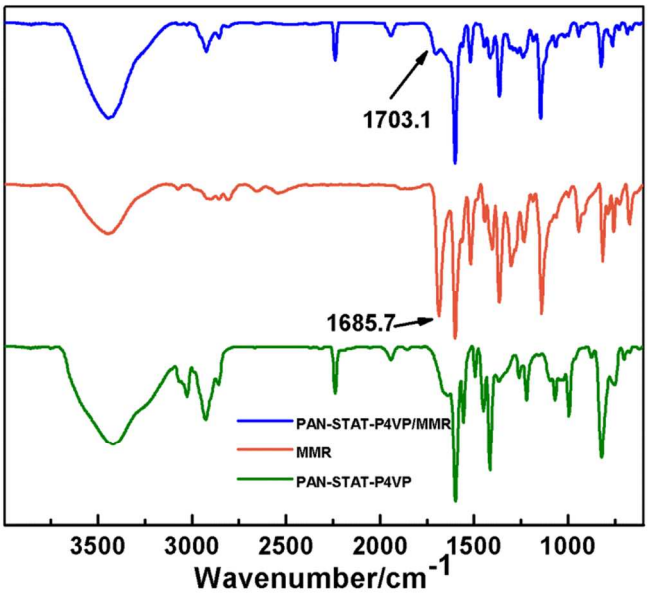

Figure 4. IR spectra of PAN_{52}-*stat*-$P4VP_{101}$, MMR and their blends PAN_{52}-*stat*-$P4VP_{101}$/MMR.

Self-assembly into thick-layer HNSs

We will now discuss the self-assembly of PAN_{52}-*stat*-$P4VP_{101}$/MMR_{41} in detail, in which each PAN-*stat*-P4VP chain has on average 41 MMR attached. The deionized water (6.1 mL, a selective solvent for pyridine moieties) was added dropwise into the THF solution (3 mL) under whisk until appearance of the faint opalescence. It indicates the formation of nano- or micro- sized particles have been generated. The HNSs were finally obtained by constantly whisk, which was carried out under ambient conditions at

room temperature. The critical steps to obtain the hollow microspheres are the procedure of constant whisk and suitable deionized water. Turbid solution was observed when the water content was in the 65 vol% under whisk. With the water content increasing from 65 to 90 vol%, hollow nanosphere structure collapsed to form colloids with solid interiors. In our previous report, the process was a net result of the hydrophilic and hydrophobic interactions between the azocomplexes and solvent molecules.

Figure 5 shows typical TEM images and SEM images of the HNSs. The samples were prepared by casting the colloidal dispersions on TEM grids and aluminum sheet dried in -40 ºC vacuum by the freeze dryer for 1 h. Meanwhile no staining treatment was performed for the observation. The TEM image of these HNSs (Figure 5a) display the integrate spheres. From the TEM image, we can estimate approximately the outer diameters of HNSs to be about 500 nm, and the inner diameters to be about 200 nm. On the other hand, the SEM image of these HNSs (Figure 5b) displays the opening of the hollow nanospheres. It means that SEM samples collapse in high voltage environment. Here we have adopted a new method to prepare the samples due to the metastable structures of the samples. We control the temperature at -40 ºC. The method retains the stability of the system through nanospheres have become opening status. This method basically sustains the spherical shape after evaporation of solvent. Meanwhile, the construction of thick-layer HNSs in SEM is in generally agreement with the TEM results

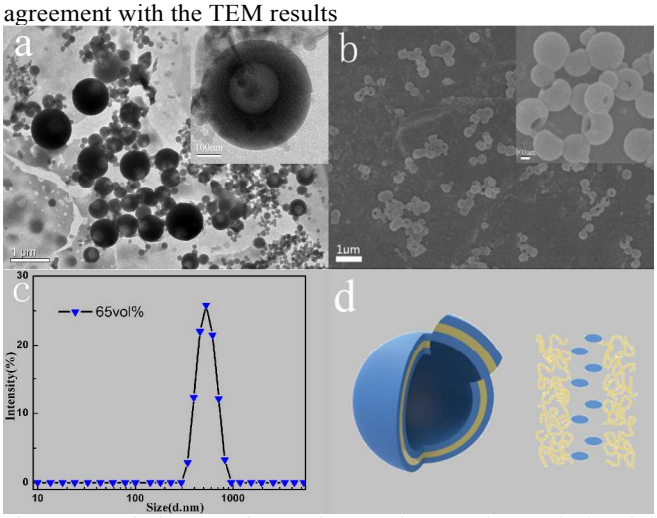

Figure 5. Typical TEM micrograph (a) and SEM micrograph (b) of the hollow microspheres of PAN_{52}-*stat*-$P4VP_{101}/MMR_{41}$. The polymer concentrations in the initial THF solutions were 1 $mg \cdot mL^{-1}$. (c) The hydrodynamic diameter for HNSs based on the azocomplexes PAN_{52}-*stat*-$P4VP_{101}/MMR_{41}$ measured by dynamic light scattering (DLS) analysis. The PDI is 0.021 for colloids formed in dispersions with water content of 65vol%. (d) a schematic illustration for the formation of the thick-layer HNSs.

The hydrodynamic diameters estimated for our HNSs by the Dynamic Light Scattering (DLS) analysis (Figure 5c) were found to be 400-600 nm. According to the Malvern specification, our samples with PDI=0.021 are considered to be monodisperse.[34] The size and its narrow distribution are in generally agreement with the TEM and SEM results. The vesicle thickness is about 150 nm, if we assume the membrane has a PAN_{52}-*stat*-$P4VP_{101}/MMR_{41}/PAN_{52}$-*stat*-$P4VP_{101}$ sandwich structure (Figure 5d).[35] In other words, within the approximations involved above, the sandwich model satisfies the experimental observations. We assume as a result of MMR hydrophobic effect, the hydrophilic group (4-VP) of PAN_{52}-*stat*-$P4VP_{101}$ is located on the membrane surface while MMR is in the middle when water content increased.

In order to further study the HNSs, we try to control the nanospheres construction. The size of the HNSs could be adjusted by changing the initial polymer concentration in THF. The relationship between the hydrodynamic diameter (Dh) and the concentration was studied by DLS (Figure 6). The PDI is 0.123, 0.021, 0.081, 0.267 and 0. 362 for hollow nanospheres formed in dispersions with initial concentration of 0.5, 1.0, 1.5and 2.0 mg/ml, respectively. When the initial concentration of PAN_{52}-*stat*-$P4VP_{101}/MMR_{41}$ changed from 0.5 to 2 $g \cdot L^{-1}$, <Dh> of the HNSs could be adjusted in a range from 390 to 1106 nm. The results show a general trend of decreasing diameter as the relative the initial polymer concentration decreases.

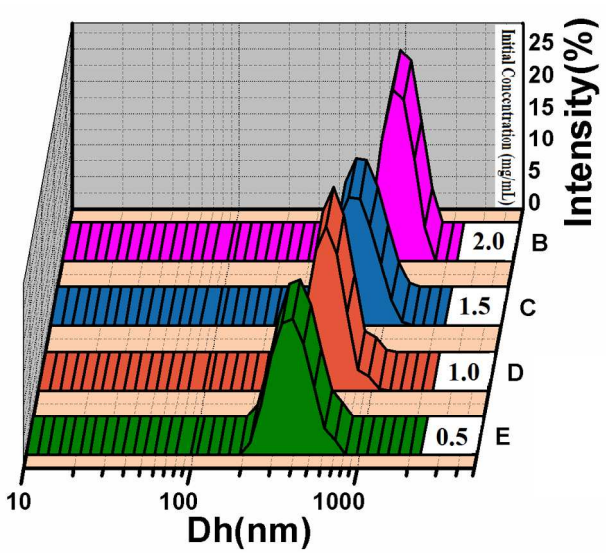

Figure 6. Relationship between the hydrodynamic diameter (<Dh>) of the HNSs and their initial polymer concentrations in THF with water content of 65vol%.

Self-assembly into thin-layer HNSs

We now discuss the self-assembly of MMR and PAN-*stat*-P4VP with a much higher MMR content, that is, PAN_{52}-*stat*-$P4VP_{101}/MMR_{91}$. The TEM (Figure 7a) and SEM (Figure 7b) images of the resulting aggregates are distinctly different from that of PAN_{52}-*stat*-$P4VP_{101}$. The TEM result presents a typical characteristic of HNSs. We can estimate approximately the diameter to be around 600nm and the thickness of the membrane to be around 60-80 nm. The thickness of HNSs composed of PAN_{52}-*stat*-$P4VP_{101}/MMR_{91}$ is thinner than HNSs composed of PAN_{52}-*stat*-$P4VP_{101}$. The SEM shows that the HNSs could basically sustain the spherical shape after evaporation of solvent. We envision that, as the content of VP is increased by hydrogen bond interaction, more copolymers will consumed by the bent bilayers because of the hydrophilic interaction between the pyridine group in the outer sphere and water molecules, which will eventually results the increase of the outer diameters. On the other hand, on the condition that PAN_{52}-*stat*-P_4VP_{101} content is fixed, with the increase of the MMR content, more VP is connected to azobenzene MMR by hydrogen bonding interaction. It would induce the decline of the hydrophilic interaction on the outer and inner surfaces of the hollow nanospheres. Meanwhile, the interaction between MMR and water, and the Van der Waals interactions among MMR moieties can enhance the hydrophobic interactions. Above all, thickness of the HNSs was compressed as a result of the combined effect of interior and exterior factors (Figure 7c).

In addition, the TEM image shows more microspheres which range from 70-80 nm than self-assembly of PAN_{52}-*stat*-$P4VP_{101}/MMR_{41}$.It attributed that MMR reunited into micelles. With the MMR content increased, an increasing number of azobenzene MMR molecules have reunited into solid microspheres.

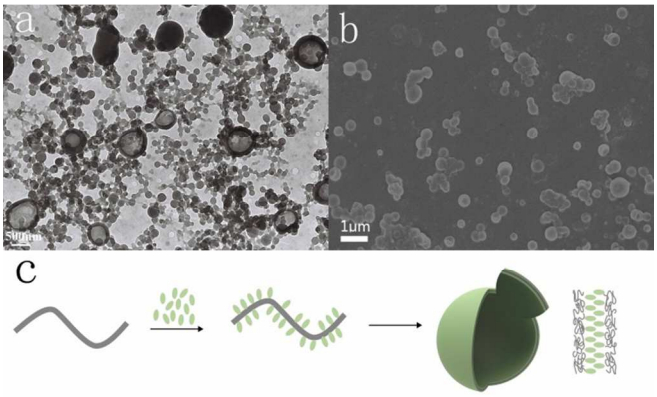

Figure 7. Typical TEM (a)micrographs and SEM. (b) micrographs of the hollow microspheres of PAN_{52}-*stat*-$P4VP_{101}/MMR_{91}$. The polymer concentrations in the initial THF solutions were 1 $mg{\cdot}mL^{-1}$. (c) a schematic illustration for the formation of the thin-layer HNSs.

The Formation Process of HNSs

In order to understand the formation process of the HNSs, we now discuss the process of intermolecular coupling. Intermolecular coupling is successfully described with the molecular exciton model: the parallel alignment of the transition dipoles shifts absorption to the blue and reduces the fluorescence rate (H-aggregate); head-to-tail alignment shifts absorption to the red and enhances fluorescence (J-aggregate) (Figure 8).[36] Early studies indicated that interesting phenomena in aggregates containing azobenzenes are J-aggregation and H-aggregation.[37] The most characteristic feature of J-aggregate is that they exhibit red-shift in the absorption spectrum with respect to the monomer absorption. The absorption spectrum of the H-aggregation consists of a blue-shifted band with respect to the monomer absorption. Hence, the spectroscopic characteristics of azo chromophores in different *stat*es can be regarded as a probe to investigate the arrangement of PAN_{52}-*stat*-$P4VP_{101}/MMR_{41}$ in aggregate according to the excition theory.

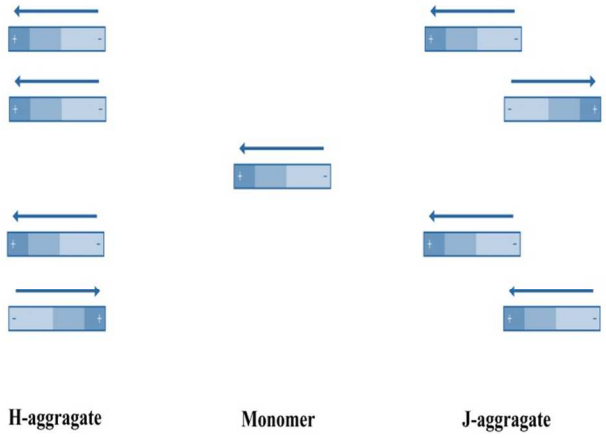

Figure 8. Schematic representation of the different arrangement of MMR dyes

To study the formation of polymeric nanospheres, a homogeneous solution was prepared by dissolving the PAN_{52}-*stat*-$P4VP_{101}/MMR_{41}$ azocomplex in THF for the preset content. Deionized water was gradually added into the complex solution under whisk. The UV-vis absorption intensity decreases as the water content increase because the concentration of the solutions decreases. The maximum absorption (max) of PAN_{52}-*stat*-$P4VP_{101}/MMR_{41}$ in THF solution (Figure 9) appears at 418 nm. λmax of PAN_{52}-*stat*-$P4VP_{101}/MMR_{41}$ in THF/H_2O mixed solution, red shifted from 418 nm to 449 nm ,while the water content increased from 0 to 90% (vol%). When the water content is low, the maximum absorption is almost 418nm and remains unchanged as the water content increases. When the water content reaches the critical values (30 vol%), the maximum absorption increases sharply. When the water content reaches the 80% (vol%), the maximum absorption remains unchanged nearly as the water content increases. The effect of J-aggregate and the alteration of solution polarity affected by the THF/H_2O mixed solvent was used to explain this phenomenon.

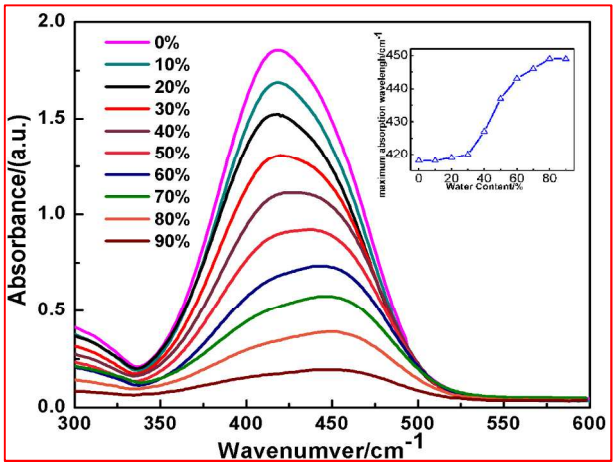

Figure 9. a) UV-Vis spectra of the PAN_{52}-*stat*-$P4VP_{101}/MMR_{41}$ azocomplexes in THF/H_2O solutions and b) the change of λmax, with the increase of water content (vol%) in the THF/H2O mixed solvents.

Figure 10 shows the UV-Vis spectra of the MMR chromophores in different stages. Whitten previously reported azobenzene chromophore shows strong evidence of "H" aggregate formation both in the pure and mixed dispersions.[38] The maximum absorption of pure MMR in DMF solution (Figure 10b) appears at 419 nm, corresponding to the π-π* transition.MMR of PAN_{52}-*stat*-$P4VP_{101}/MMR_{411}$ shows an evidence of "H" aggregate formation in THF solution. While the water content reaches 70% (vol%), λmax of PAN_{52}-*stat*-$P4VP_{101}/MMR_{41}$ is 446 nm, which is longer than that of the MMR in pure water (445 nm).When the water content reaches 90% (vol%), the further red-shift of the absorption wavelength suggested the presence of J-aggregation of dyes.

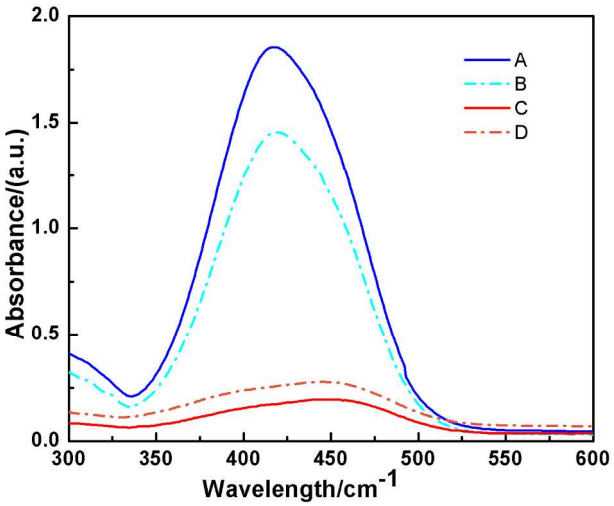

Figure 10. UV–Vis spectra of: (a) PAN_{52}-*stat*-$P4VP_{101}$/MMR_{41} in THF, (b) MMR in THF, (c) PAN_{52}-*stat*-$P4VP_{101}$/MMR_{41} in THF/H_2O (9:1) mixed solution and (d) MMR in aqueous solution.

We propose a mechanism, as the water content increases, the solubility of the PAN_{52}-*stat*-$P4VP_{101}$/MMR_{41} azocomplex becomes poorer for the hydrophobic groups (MMR and AN), inducing the aggregation of the polymer chains and MMR moieties. UV–Vis spectra indicated that MMR dyes could form different dye-dye aggregates and show metachromacy in aqueous via J-aggregation.

To investigate further, we turned to track the formation of the HNSs. The dynamic light scattering (DLS) can supply further information about the aggregate formation. As mentioned above, the aggregate formation process was controlled by adjusting the water content of the medium with the addition of the deionized water into the dispersion under whisk. After one addition, the dispersion was set aside for a period of time. A series of dispersions with water content in the range from 65 vol% to 90 vol% were obtained by this dynamic evolution process. Then, mixtures of H_2O and THF with the same water contents were slowly added into the polymer dispersions to dilute them to suitable concentrations. The hydrodynamic diameter (D_h) and polydispersity of aggregates formed in the aqueous dispersions were monitored by DLS after each water content interval. Figure 11 gives D_h distributions of aggregates formed at the different stages with an initial polymer concentration of 1 mg·mL^{-1}, which were measured at the scattering angle of 90º. As the water content increased, $<D_h>$ of the polymeric aggregates undergoes a significant decrease from 531 nm to 190 nm with almost unchanged PDI in range 0.010-0.115. It shows that the polymeric aggregates, existing in the dispersion with water content of 65 vol%, have characteristics of loose aggregates. If excess water is added at this stage, the loosely associated polymer chains collapse to form colloids with solid interiors through hydrophobic interactions.[39] The method could avoid the loose aggregates amalgamating with each other.

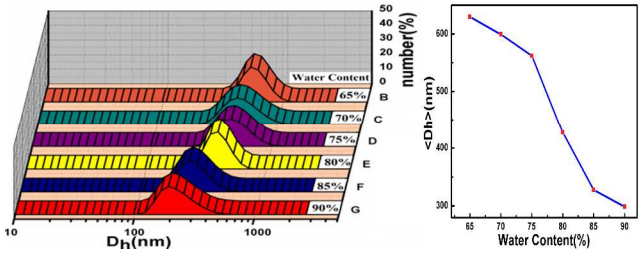

Figure 11. Hydrodynamic diameter (D_h) and its distribution for polymeric aggregates formed in H_2O–THF media with different water contents. The initial concentration of PAN_{52}-*stat*-$P4VP_{101}$ /MMR_{41} in THF was 1 mg·mL^{-1}. After the required amounts of water were slowly added into the stock solutions, the dispersions were diluted to ~10 mL by adding H_2O–THF media with the same water contents. The PDI is 0.010, 0.081, 0.081, 0.028, 0.196 and 0. 115 for colloids formed in dispersions with water content of 65, 70, 75, 80, 85and 90 vol%, respectively.

Here we put forward a kind of mechanism to explain the formation of HNSs. A schematic illustration of self-assembly process is shown in Figure 12, which is a net result of the hydrophilic and hydrophobic interactions between the azocomplexes and solvent molecules, and also the bending energy of bilayers (i.e., the energy cost for bending the bilayers). Firstly, azocomplexes were expected to form through hydrogen bonds between the carboxyl group at the MMR and the pyridine group of PAN-*stat*-P4VP by mixing MMR and PAN-*stat*-P4VP under whisk. When the deionized water was added into a polymer solution of THF, the hydrophobic interactions between MMR and water, and the Van der Waals interactions among MMR moieties induce the formation of a bilayer-like intermediate structure of the azocomplexes, with the hydrophilic pyridine groups staying on the two surfaces of the bilayers. As the water content further increased, hydrophobic groups tended to aggregate together by the chain segment movement and hydrophilic groups were located in the exterior of hydrophobic groups facing the outside water. Under the condition of stirring constantly, with the appearance of the faint opalescence, it indicates the nano- or micro-sized particles have been generated. The bilayers are bended over to form HNSs, where the hydrophilic groups are located in the outer and inner surfaces of the HNSs. The red-shift of λ_{max} for the azo-dyes was observed due to the J-aggregation of MMR in the bilayer interior. However, the shell is thicker than bilayer model in real systems. This phenomenon was attributed to the rigidity structure of MMR which impedes the close contact of bilayer. So, the phenomenon of red-shift is not obvious. With the further addition of water, hollow nanospheres collapse to form colloids with solid interiors through hydrophobic interactions.

Conclusions

In summary, a novel method based on non-covalent bond self-assembly technology was provided hollow nanospheres with azo functional groups. Azocomplex nanospheres with diameter of 300~1000nm were obtained by the H-bond (non-covalently) self-assembly of poly (acrylonitrile-*stat*-4-vinylpyridine) (PAN-*stat*-P4VP) and azobenzene m-Methyl red (MMR) in the aqueous solvents. Polymeric hollow nanospheres with azobenzene chromospheres were formed in THF/H_2O mixed solvent, with 65 vol% H_2O in mass. As the solution was stirred constantly, mixing dilute solutions of MMR and PAN-*stat*-P4VP led to faint opalescence that indicated the nano-sized particles. This method of hollow nanospheres preparation, the addition of doping agent and templates, the further calcinations or chemical etching process are avoided. Besides, these hollow nanospheres have potential optical property due to the azobenzene group, such as photoinduced deformation. Consequently, the azobenzene-containing hollow nanospheres have a wide range of applications value in the field of photoelectric materials and biological medicine.

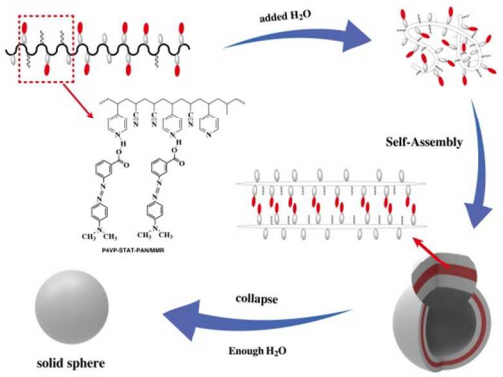

Figure 12. Schematic illustration for the formation process of PAN-*stat*-P4VP/MMR hollow nanospheres

Notes and references

[a]Key Laboratory of Green Chemistry and Technology and College of Chemistry, Sichuan University, Chengdu, China, Tel.: +86 28 85418112; fax: +86 28 85412907 E-mail: changer@scu.edu.cn

Electronic Supplementary Information (ESI) available: [details of any supplementary information available should be included here]. See DOI: 10.1039/b000000x/

1 C. J. Barrett, J. I. Mamiya, K. G. Yager and T. Ikeda, *Soft Matter*, 2007, **3**, 1249-1261.
2 S. C. Sebai, D. Milioni, A. Walrant, I. D. Alves, S. Sagan, C. Huin, D. Massotte, S. Ccribier and C. Tribet, *Angew. Chem. Int. Ed.*, 2012, **124**, 2174-2178.
3 G. Wang, M. Zhang, T. Zhang, J. Guan and H. Yang, *RSC Adv.*, 2012, **2**, 487-493.
4 D. J. Coady, D. M. Khramov, B. C. Norris, A. G. Tennyson, and C. W. Bielawski, *Angew. Chem. Int. Ed.*, 2009, **48**, 5187-5190.
5 Y. Yu, M. Nakano, and T. Ikeda, *Nature*, 2003, **425**, 145-145.
6 T. Ueki, Y. Nakamura, A. Yamaguchi, K. Niitsuma, T. P. Lodge, and M. Watanabe, *Macromolecules*, 2011, **44**, 6908-6914.
7 G. Fang, N. Koral, C. H. Zhu, Y. Yi, M. A. Glaser, J. E. Maclennan, N. A. Clark, E. D. Korblova and D. M. Walba, *Langmuir*, 2011, **27**, 3336-3342.
8 N. Zettsu, T. Ogasawara, N. Mizoshita, S. Nagano, and T. Seki, *Adv. Mater.*, 2008, **20**, 516-521.
9 Z. Chen, C. Zhong, Z. Zhang, Z. Li, L. Niu, Y. Bin, F. Zhang, *J. Phys. Chem. B*, 2008, **112**, 7387-7394.
10 W. Wang, X. Sun, W. Wu, H. Peng, and Y. Yu, *Angew. Chem. Int. Ed.*, 2012, **124**, 4722-4725.
11 D. H. Han, X. Tong, Y. Zhao, T. Galstian, and Y. Zhao, *Macromolecules*, 2010, **43**, 3664-3671.
12 C. J. Barrett, J Mamiya, K. G. Yager and T. Ikeda, *Soft Matter*, 2007, **3,** 1249-1261.
13 Z. H. Shi, D. Chen, H. Lu, B. Wu, J. Ma, R. Cheng, J. Fang and X. Chen, *Soft Matter*, 2012, **8**, 6174-6184.
14 L. Zhang and A. Eisenberg, *Science*. 1995, **268**, 23.
15 L. Zhang and A. Eisenberg, *J. Am. Chem. Soc.*, 1996, **118**, 3168-3181.
16 D. E. Discher and A. Eisenberg, *Science*, 2002, **297**, 967-973.
17 L. Ziserman, H. Y. Lee, S. R. Raghavan, A. Mor and D. Danino, *J. Am. Chem. Soc.*, 2011, **133**, 2511-2517
18 Z. Xing, C. Wang, J. Yan, L. Li and L. Zha, *Soft Matter*, 2011, **7**, 7992-7997.
19 Y. Zhao, and L. Jiang, *Adv. Mater.*, 2009, **21**, 3621-3638.
20 B. G. De Geest, N. N. Sanders, G. B. Sukhorukov, J. Demeester and S. C. De Smedt, *Chem. Soc. Rev.*, 2007, **36**, 636-649.
21 (a) Z. Sun, F. Bai, H. Wu, S. K. Schmitt, D. M. Boye and H. Fan, *J. Am. Chem. Soc.*, 2009, **131**, 13594-13595. (b) G. Fu, G. Li, K. G. Neoh and E. T. Kang, *Prog. Polym. Sci.*, 2011, **36**, 127-167. (c) I. W. Hamley, *Soft Matter*, 2005, **1**, 36-43.
22 J. Liu, Y. He and X. Wang, *Langmuir*, 2008, **24**, 678-682.
23 H. Lu, J. Wang, Y. Lin and J. Cheng, *J. Am. Chem. Soc.*, 2009, **131**, 13582-13583.
24 (a) D. Wang, G. Ye, Y. Zhu and X. Wang, *Macromolecules*, 2009, **42**, 2651-2657. (b) S. Deshmukh, L. Bromberg, K. A. Smith and T. A. Hatton, *Langmuir*, 2009, **25**, 3459-3466. (c) M. Aoyama, J. Watanabe and S. Inoue, *J. Am. Chem. Soc.*, 1990, **112**, 5542-5545. (d) Y. Li, Y. He, X. Tong and X. Wang, *Langmuir*, 2006, **22**, 2288-2291.
25 C. Jin, T. Zhang, F. Liu, L. Wang, Q. Yin and D. Q. Xiao, *RSC Adv.*, 2014, **4**, 8216-8223.
26 Y. Wang, P. Han, H. Xu, Z. Wang, X. Zhang and A. V. Kabanov, *Langmuir*, 2009, **26**: 709-715.
27 C. Jin, Y. Zhao, H. Wang, K. Lin and Q. Yin, *Colloid Polym. Sci.*, 2012, **290**, 741-749.
28 P. Liang and A. B. Pardee, *Science*, 1992, **257**, 967-971.
29 G. E. Southard, K. A. Van Houten, E. W. Ott Jr and G. M. Murray, *Anal. Chim. Acta.,* 2007, **581**, 202-207.
30 H. Duan, D. Chen, M. Jiang, W. Gan, S. Li, M. Wang and J. Gong, *J. Am. Chem. Soc.*, 2001, **123**, 12097-12098.
31 (a) M. Wang, M. Jiang, F. L. Ning, D. Chen, S. Liu and H. Duan, *Macromolecules*, 2002, **35**, 5980-5989. (b) Y. Zhao, F. J. Sakai, L. Su, Y. Liu, K. Wei, G. Chen and M. Jiang, *Adv. Mater.*, 2013, **25**, 5215-5256. (c) M. Kuang, H. Duan, J. Wang, D. Chen and M. Jiang, *Chem. Commun.*, 2003, **4**, 496-497.
32 L. He, E. S. Read, S. P. Armes and D. J. Adams, *Macromolecules*, 2007, **40**, 4429-4438.
33 D. Xie, M. Jiang, G. Zhang and D. Chen, *Chem. - Eur. J.*, 2007, **13**, 3346-3353.
34 X. Zhang, B. Xia, H. Ye, Y. Zhang, B. Xiao, L. Yan, H. Lv and B. Jiang, *J. Mater. Chem.*, 2012, **22**, 13132-13140.
35 C. Mu, Y. Yu, R. Wang, K. Wu, D. Xu and G. Guo, *Adv. Mater.*, 2004, **16**, 1550-1553.
36 (a) J. Cornil, D. Beljonne, J. P. Calbert and J. L. Brédas, *Adv. Mater.*, 2001, **13**, 1053-1067. (b) S. Ito, H. Miura, S. Uchida, M. Takata, K. Sumioka, P. Liska, P. Comte, P. Péchy and M. Grätzel, *Chem. Commun.*, 2008, **41**, 5194-5196. (c) B. K. An, S. K. Kwon, S. D. Jung and S. Y. Park, *J. Am. Chem. Soc.*, 2002, **124**, 14410-14415.
37 D. Han, X. Tong, Y. Zhao, T. Galstian and Y. Zhao, *Macromolecules*, 2010, **43**, 3664-3671. (b) X. Song, J. Perlstein and D. G. Whitten, *J. Am. Chem. Soc.*, 1997, **119**, 9144-9159. (c) T. Kawai, J. Umemura and T. Takenaka, *Langmuir*, 1989, **5**, 1378-1383.(d) R. M. Tejedor, M. Millaruelo, L. Oriol, J. L. Serrano, R. Alcalá, F. J. Rodríguez and

B. Villacampa, *J. Mater. Chem.*, 2006, **16**, 1674-1680. (e) L. Zhang, J. M. Cole and X. Liu, *J. Phys. Chem. C*, 2013, **117**, 26316-26323.

38 J. M. Kuiper and J. B. F. N. Engberts, *Langmuir*, 2004, **20**, 1152-1160.

39 (a) Y. Li, Y. He, X. Tong and X. Wang, *J. Am. Chem. Soc.*, 2005, **127**, 2402-2403. (b) N. Li, G. Ye, Y. He and X. Wang, *Chem. Commun.*, 2011, **47**, 4757-4759.

